DSTO

Investigation into the Effects of Underwater Shock Waves on Simple Structures, Shielded and Bare Explosive Materials

Michael Chung and Trevor Kinsey

DSTO-RR-0134

] APPROVED FOR PUBLIC RELEASE

DEPARTMENT ◆ OF DEFENCE

DEFENCE SCIENCE AND TECHNOLOGY ORGANISATION

Investigation into the Effects of Underwater Shock Waves on Simple Structures, Shielded and Bare Explosive Materials

Michael Chung and Trevor Kinsey

Weapons Systems Division
Aeronautical and Maritime Research Laboratory

DSTO-RR-0134

ABSTRACT

The detonation of an underwater charge creates a shock wave and a bubble of gaseous products at high temperature and pressure. At greater ranges, the shock wave and bubble become separated and their effects on structures may be studied separately. However, close to the point of detonation, in the regions typically used for sea-mine neutralisation, the shock wave and bubble lie in close proximity and their relative importance in the neutralisation process is not known. A series of scaled experiments to visualise the early development of the shock wave and bubble, and their interactions with an explosive and with simple structures were devised. These experiments used spherical pentolite charges and cylindrical Composition B charges as the donor and acceptor charges respectively. Both charges were suspended in a small, transparent water-filled tank and the effects of the exploding donor recorded by a Cordin rotating mirror camera.

The results show that the underwater shock wave is the principle cause of damage in the near field and initiates detonation in the explosive material long before the bubble contacts the explosive.

RELEASE LIMITATION

Approved for public release

DEPARTMENT OF DEFENCE

DEFENCE SCIENCE AND TECHNOLOGY ORGANISATION

Published by

DSTO Aeronautical and Maritime Research Laboratory
PO Box 4331
Melbourne Victoria 3001 Australia

Telephone: (03) 9626 7000
Fax: (03) 9626 7999

AR-010-571
June 1998

APPROVED FOR PUBLIC RELEASE

Investigation into the Effects of Underwater Shock Waves on Simple Structures, Shielded and Bare Explosive Materials

Executive Summary

Mine Hunter Coastal Project Director requires a predictive capability to assess the effect of mine disposal charges against current and future threat mines in various marine environments.

As a consequence of this requirement, it is necessary to evaluate factors that determine the sympathetic distance between generic disposal charges and mine type charges.

To develop analytical methods for predicting sympathetic detonation of sea mines, a series of scaled experiments were devised to visualise the interaction of an underwater explosion with an explosive material and various simple structures.

The detonation of a spherical pentolite charge and the expansion of the shock wave and bubble were recorded by a rotating mirror, simultaneous streak and framing camera. The interaction of the underwater shock wave and bubble with an explosive acceptor was investigated and, to determine attenuation effects of sea-mine casings, the interaction of a shock wave with a steel plate and perspex sheet was also investigated.

The velocity of the shock wave incident onto these simple targets was determined from streak records. These results show that the shock impedance of perspex sheet is negligible when compared with that of steel. The dishing of the steel plate caused by the underwater explosion was measured, using both the film record and the plate recovered after the event. These results compared favourably.

The camera was also used to study experiments with explosive acceptors. Two types of reaction in Composition B acceptors were achieved by varying the separation between donor and acceptor charge. At lesser distances, the passage of the underwater shock wave initiated detonation in the acceptor. This reaction was characterised by the luminous detonation wave in the acceptor and the propagation of a shock wave into the surrounding water. At greater separations a lower order reaction occurred. Inclusion of a perspex sheet shielded the charge from the bubble without attenuating the shock wave sufficiently to prevent initiation of detonation in the acceptor charge.

The scaled experiments show that even close to a detonating underwater charge, the shock wave and bubble have separated sufficiently to produce individual effects on explosives and simple structures. The results show that an underwater shock wave will initiate detonation in an explosive material long before the bubble makes contact with the explosive material.

These results will allow near field and far field properties of an underwater shock wave to be evaluated and the effectiveness of the shock wave against generic sea-mines to be empirically modelled.

As a consequence of this model, Navy will be able to predict the outcome of mine clearing operations from knowledge of;

1. the explosive filling in the clearing charge and sea mine,
2. the stand-off distance between clearing charge and sea mine and,
3. the material properties of the sea mine's casing.

Authors

Michael Chung
Weapons Systems Division

Michael Chung joined DSTO in 1969 and has worked widely in the fields of Applied Physics at AMRL. Recent work has investigated the effects produced by the interaction of underwater shock waves with explosive materials and simple structures. He is an Associate of the School of Mines Ballarat and graduated from the Royal Melbourne Institute of Technology in Applied Physics.

Trevor Kinsey
Weapons Systems Division

Trevor Kinsey graduated from the Royal Melbourne Institute of Technology, with a Bachelor of Applied Science in Photography in 1981. Since then he has worked at MRL specialising in the field of explosives photoinstrumentation. His principal areas of work in that time have ranged from initiation and detonation studies to fragmentation and ship shock testing.

Contents

1. Introduction

Underwater detonation of large explosive charges is a common method of attack against ships or submarines and at present, is the principal method of neutralising sea mines. The shock wave and bubble produced by the expansion of the detonation products are the principal damage mechanisms of an underwater explosion and each affects the target in a different manner. At greater ranges, the expanding shock wave and bubble become separated because of the shock wave's greater velocity and as a result, the target will be subjected in turn, to each effect. The combined effects can be devastating to the hull of a vessel and several countries have initiated special vulnerability studies to quantify the effects of underwater explosions.

However, sea mines are cleared by the detonation of charges placed either close by or in contact with the mines. At these separations, a shock wave and a bubble of detonation products at high temperature and pressure exist in close proximity and the relative importance of each of these effects in the clearing process is not known. Computations made for the detonation of a small pentolite sphere [1] have shown that the shock wave and bubble have clearly separated after 3 charge radii, and aquarium experiments [2] with pentolite donors and high explosive acceptors show a reaction is initiated in the acceptor charge by the passage of a shock wave. From this work, one may conjecture that the underwater shock wave alone may be the main cause of initiation.

Previous experiments have determined the maximum separation distance for the underwater sympathetic detonation of acceptor charges and enabled the velocity of the shock wave within three charge radii of the donor to be estimated [3]. Unfortunately, these experiments did not indicate the involvement, if any, of the hot gaseous products in the detonation process of the acceptor or the period over which initiation and build-up to detonation of the acceptor have occurred.

To aid in the development of analytical methods for predicting sympathetic detonation of sea mines, the response of the acceptor charge to the gaseous products and the period of shock loading, prior to detonation break-out, need to be clarified. Consequently, in the light of Liddiard and Forbes's underwater sensitivity tests [2], a series of scaled experiments to visualise the interaction of an underwater explosion with an acceptor and various simple structures was devised. This paper presents the results of the study.

2. Theory.

The characteristics of shock waves propagating through a medium may be determined by simple analytical means. The pressure P of a shock wave of velocity U, travelling in a medium of density ρ, is given by [4];

$$P - P_0 = \rho u U \qquad (1)$$

where u is the particle velocity of the shock wave and P_0 is the ambient pressure in the medium.

The relationship between U and u in a medium is detemined experimentally and in the case of water, is given by [5];

$$U = 1.483 + 25.306 \log_{10}[1 + \frac{u}{5.19}] \qquad (2),$$

where U and u are in km/s.

From experimental measurements of U, u may be calculated from (2) and the pressure of the shock wave in a medium of density ρ, calculated from (1).

When a shock wave interacts with a boundary between two media, a reflected shock wave is produced in one medium and a transmitted shock is produced in the other. By the principles of the conservation of energy and momentum, the pressure and particle velocity across the boundary are continous and by using impedance matching techniques, the characteristics of the reflected and transmitted waves may be calculated [4].

The simple methods described above are assumed to apply to the near field of an exploding donor, a region less than 5 charge radii from the donor.

3. Experimental Details.

The experiments were conducted in a small scale test facility shown schematically in Figure 1. This facility utilised a firing chamber designed for a maximum 2.25 kg charge mass, a Cordin model 330 rotating mirror camera and a transparent aquarium, illuminated by an Argon light bomb. The chamber has 7 viewing ports in the horizontal plane of the charge. These allow flexibility in the geometrical arrangement of the aquarium and the optimisation of the light path through the chamber. The Cordin model 330 rotating mirror camera is a simultaneous streak and framing camera, giving good temporal resolution from the streak records, and good pictorial representation of the event from the framing records. When taken together, the two forms of record give a better understanding of the event.

Spherical pentolite donor charges of mass 0.5 kg and radius 4.2 cm were used for all experiments. These charges were centrally initiated by an EBW detonator to ensure that a spherical shock wave and bubble were produced. Cylindrical Composition B charges, 60 mm diameter and 120 mm long were used as acceptor charges.

The explosive charge and target were positioned in the aquarium and rigidly supported in the Cordin camera's field of view. The camera was arranged to view the subject via an image rotator and two mirrors. The first of these mirrors was front surface coated to provide better image quality and was mounted on a stand outside the firing cell. The second was placed inside the firing cell and was expected to be destroyed with every shot. The firing cell window was a sheet of 25 mm thick PMMA, faced on the inside with a disposable 3 mm thick sheet of PMMA.

Figure 1. Schematic of the small scale test facility.

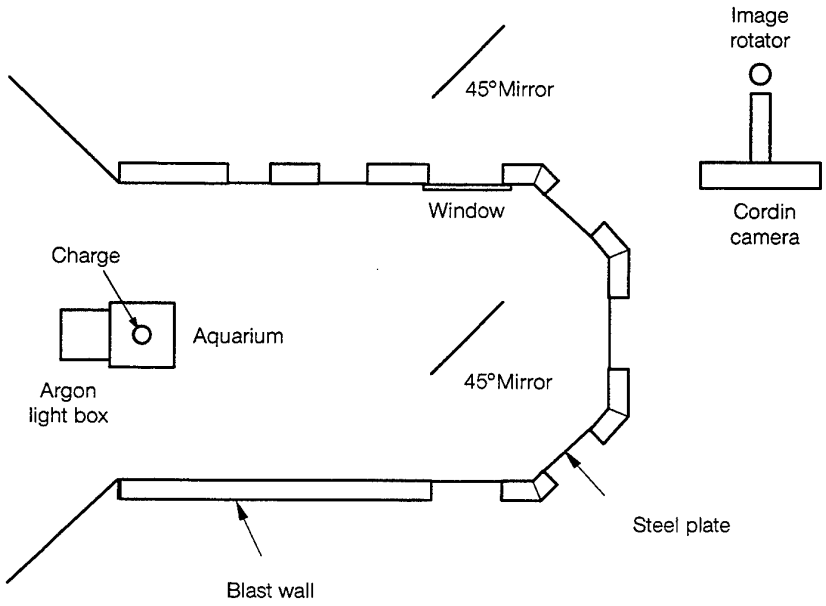

The subject was back illuminated by an explosive/Argon light bomb. This was a 500 mm cube (minus one side), manufactured from cardboard silvered on one side with aluminium. A 200 mm square charge of approximately 340g of PE4 explosive was used to drive the light source. Exploding Bridge Wire (EBW) detonators (RISI 501) were used to initiate the flash bomb, these detonators were selected for performance, safety and reliability of functioning. After a delay of 25-30 μs, to allow the light to build in intensity, the pentolite charge was fired.

A layer of tracing paper, taped to the back of the aquarium, was used to diffuse to the light. The cube was filled with welding grade Argon prior to firing. The size of the light bomb and driver charge were determined by experiment. The height and width were dictated by the field of view of the camera, and the length was chosen to provide light of a suitable intensity for the duration required. The design of the light bomb was not optimised, rather, once an effective device had been found no further development work was carried out. It is likely that improvements could be made to the design.

Prior to the fixing of the light bomb to the back of the aquarium, a grid pattern was attached to the back face of the aquarium using printed circuit board layout tape (3 mm wide) generally with a spacing of 100 mm. Allowing for parallax error, this provided a ready reference on each frame and on the streak record. The pentolite sphere, which was of a known diameter, provided a scale reference in the plane of the experiment for the film records.

All events were recorded on Kodak T-max P3200 35mm black and white film, processed for 11 minutes at 30 deg C in Kodak T-max RS developer in a rotary tube processor to obtain maximum film speed.

The framing records produced by the Cordin camera were used to visualise the interaction of the underwater shock wave with the explosives and simple structures whilst the streak records were used to determine displacement data of the shock wave and bubble surface. The diameter of the spherical donor charge was taken as the axis of symmetry for the aquarium and, by positioning the streak camera's slit across the diameter, the symmetrical expansion of the shock wave and bubble surface allowed two paths of the shock wave and bubble surface to be tracked. These paths were digitised and plotted in the distance-time domain. The velocity of expansion of either the shock wave (U) or bubble may be determined at any point by calculating, at that point, the gradient of the distance-time curve.

4. Results and Discussion

Results are obtained from the framing and streak records from knowledge of the geometry of the camera and the speed of the rotating mirror. The number of frames per second F and the nominal writing speed W of the camera may be calculated from the following equations;

$$F = \frac{2.4 * 10^8}{P} \qquad (3) \text{ and,}$$

$$W = \frac{1276.8}{P} \quad mm/\mu s \qquad (4)$$

respectively where P is the cameras turbine speed in μs.

The details of the framing and streak records are shown in Table 1.

Table 1. Camera settings.

Experiment described in Section :	Nominal turbine speed μs	Frames/second	Writing speed $mm/\mu s$
4.1	240.1	10^6	5.318
4.2	480.1	$0.5*10^6$	2.659
4.3	240.1	10^6	5.318
4.4	479.8	$0.5*10^6$	2.661
4.5	480.1	$0.5*10^6$	2.659

Calculations of the velocity of detonation of the Composition B receptor from the streak records in Sections 4.3 and 4.5 are 8600 m/s and 11250 m/s respectively whilst an accepted value of the velocity of detonation of Composition B is 8030 m/s [6]. Clearly, the correlation between calculated and reference velocities of detonation for the turbine speed of 480 μs is poor.

The experimental method and method of analysis of results were reviewed and no reason could be found to explain the difference between measured and reference velocities of detonation. As the Cordin camera was overdue for servicing, it was considered that the turbine was not operating correctly at these higher speeds and velocity calculations made in Sections 4.2, 4.4 and 4.5 should be corrected by the scaling factor 8030/11250 (ie 0.7).

Experimental errors were taken as 7%, which is the difference between the velocity of detonation calculated in Section 4.3 (8600 m/s) and the reference velocity (8030 m/s).

4.1 Detonation of a spherical charge

The near-field expansion of the underwater shock wave and gaseous products from an exploding charge, unimpeded by acceptor explosives or simple structures, are detailed by the streak and framing records shown in Figure 2.

The streak record shows the arrival of the luminous detonation wave at the surface of the spherical charge and the development of both the shock wave and the bubble of detonation products. This record clearly details the rapid expansion of the detonation products, the expansion of the underwater shock wave and the development of the bubble of detonation products. The rapid expansion of the products lasts until the emergence of the shock wave, after which the bubble's expansion slows because it is no longer driven by the energy of the detonation wave but by the internal energy of the gaseous products from the explosion.

As the shock wave expands, it produces a transparent sphere of shocked water with a different refractive index to that of the surrounding water. This created a large 'lens' and its effect on transmitted light is evident by the distortion of the background grid lines when viewed through the spheroid. This effect is shown in Figure 2c.

The expansion of both the shock wave and the bubble's surface was digitised from the streak record and their paths in the distance-time domain are shown in Figure 3. The initial surface of the sphere was used as the reference from which distances were measured. Because of the difficulty in digitising the streak record, a common time zero could not be chosen for the expansion of the shock wave and bubble from both sides of the viewing slit. Consequently, Figure 3 presents only the expansion of the shock wave and bubble surface from one side of the streak camera's viewing slit.

Figure 2. Streak record (a) and framing records of the detonation of a spherical, pentolite charge (b) 7 μs and (c) 25 μs after initiation.

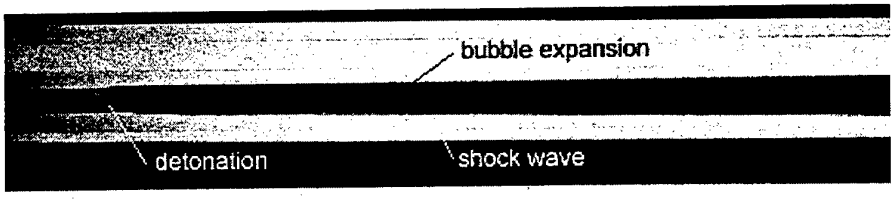

a

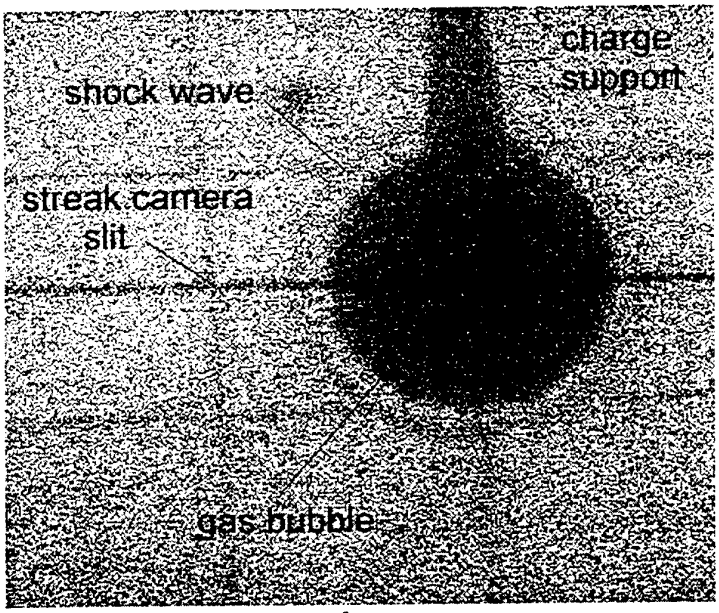

b

c

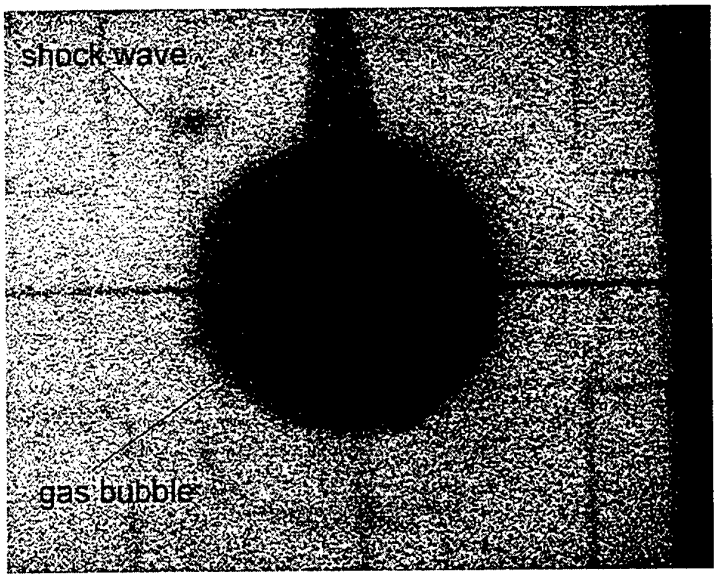

Figure 3. Expansion of the shock wave and bubble surface in the distance-time domain.

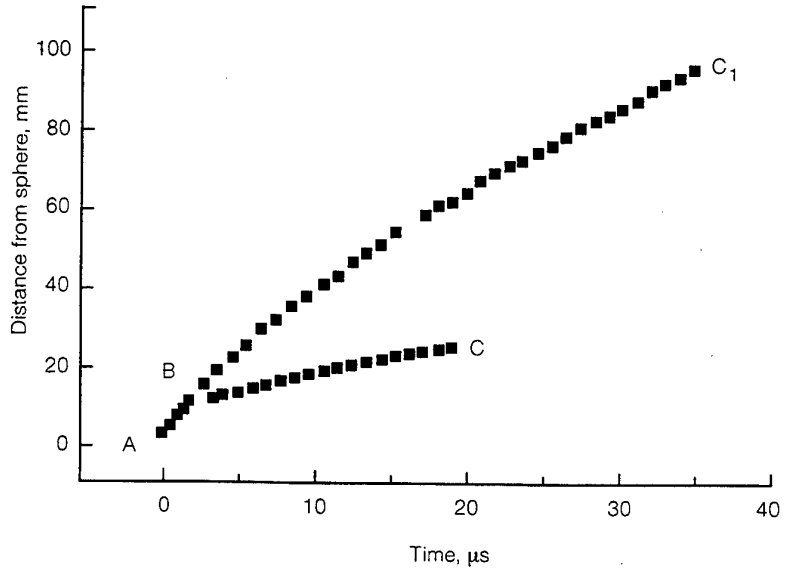

Figure 3 shows the rapid initial expansion of the detonating pentolite sphere (section AB) and the shock wave (section BC1) rapidly separating from the bubble of detonation products (section BC).

Calculating the gradient of the curves shown in Figure 3 enables the velocity of expanding shock wave and bubble to be determined over the first 35 μs of the event. Ideally, for no energy losses to the surrounding medium, the properties of a small amplitude spherical shock wave are inversely proportional to the radial distance from the source of the shock wave [7]. Consequently, a power curve of best fit is the most appropriate function that should be used to model the relationship between velocity and radial distance. The variation in shock wave velocity U with reduced distance R from the surface of the donor charge is shown in Figure 4. The use of reduced distance as the second variable allows velocities to be scaled for explosive charges whose mass is other than 0.5 kg and the reduced distance is defined as;

$$R = s / m^{\frac{1}{3}},$$

where s is the distance from the surface of the charge in mm and m is the mass of the charge in kg.

Figure 4. Variation in velocity of expansion of the shock wave, with reduced distance.

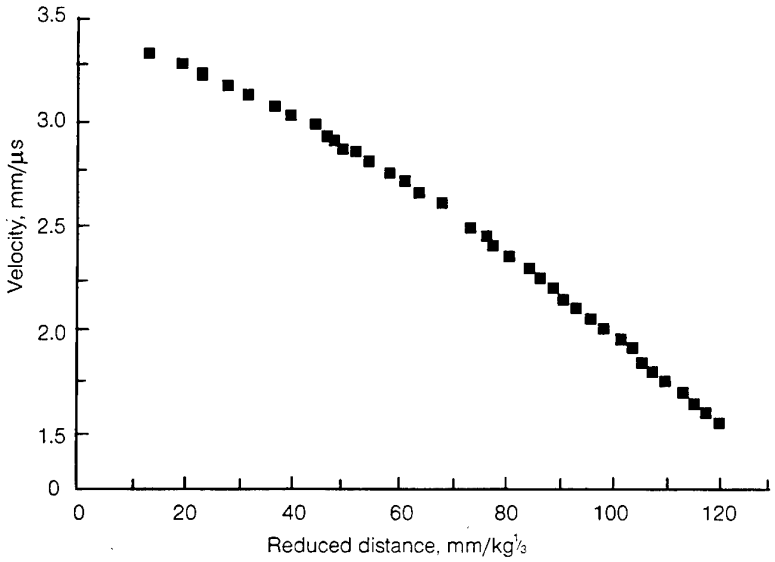

Figure 4 shows that the velocity of the shock wave rapidly decreases with distance and has dropped to approximately 1.5 $mm/\mu s$ (the acoustic velocity in water), after the shock wave has moved a distance of 2.3 charge radii (120 $mm/kg^{\frac{1}{3}}$) from the reference surface of the donor charge.

The power curve of best fit for the data described by the curve in Figure 4 is given by;

$$U = 11.33R^{-0.37} \qquad (5)$$

Here, U is the velocity of the shock wave in $mm/\mu s$. The coefficient of determination for this curve is 0.83.

This relationship shows that the velocity reduces much more rapidly with distance than that predicted by the inverse square law. This rapid reduction in velocity may be due to significant energy losses to the surrounding water which would; possibly change its state from a liquid to a gas, raise the temperature of the water and increase its initial momentum.

The variation in velocity of expansion of the bubble's surface with reduced distance is shown in Figure 5. Here, the average velocity of expansion of the detonating sphere is approximately 4.6 ± 0.3 $mm/\mu s$ and the velocity of the sphere is seen to decrease from 6.0 ± 0.4 $mm/\mu s$ to 1.0 ± 0.07 $mm/\mu s$ over a reduced distance of approximately 10 $mm/kg^{\frac{1}{3}}$. By this time, the shock wave has emerged from the bubble of detonation products and the bubble's velocity of expansion should only be determined by the temperature and pressure within, and the external pressure on, the bubble. Under

these conditions, the velocity of expansion of the bubble decreases from 1.0 ± 0.07 $mm/\mu s$ to 0.56 ± 0.04 $mm/\mu s$ whilst the bubble radius increases from 55.0 mm to 67.0 mm.

Figure 5. Variation in velocity of bubble expansion with reduced distance.

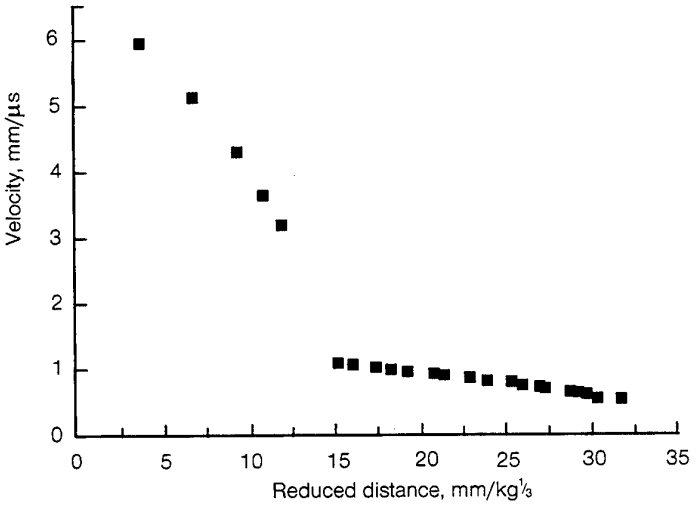

4.2 Interaction of a shock wave with simple structures.

Figure 6 illustrates the interaction of a shock wave with a steel plate and perspex sheet. A pentolite donor was suspended between the plate and sheet and detonated. On recovery, the steel plate was found to be dished and the perspex sheet, pulverised.

The streak record shows multiple reflections of the shock wave between the steel plate and the expanding bubble and also a transmitted wave through the plate. The steel plate is seen to be responding to the incident shock wave and the transmitted shock wave clears the plate approximately 18 μs after initial contact. The mechanism of the steel plate's response to the passage of the shock wave is not clear, it could be due to either localised motion of the plate (hence distortion) or the motion of embedded particles on the plate. Because of this uncertainity, the plates 'response' was not considered suitable for digitising and only the paths of the incident and transmitted shock waves were considered. These paths in the distance-time domain are shown in Figure 7.

Figure 6. Streak record (a) and framing records of the interaction of a shock wave with a steel plate and perspex sheet, (b) 4 μs and (c) 8.5 μs after initiation of the donor charge.

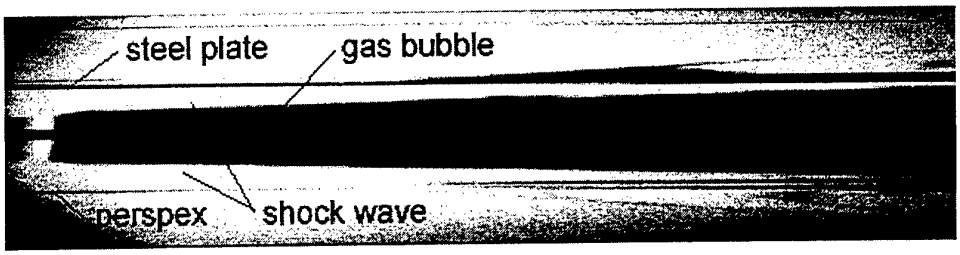

a

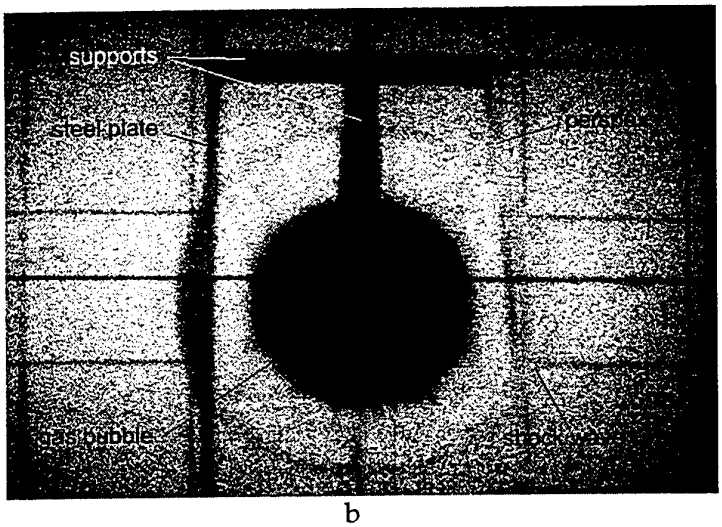

b

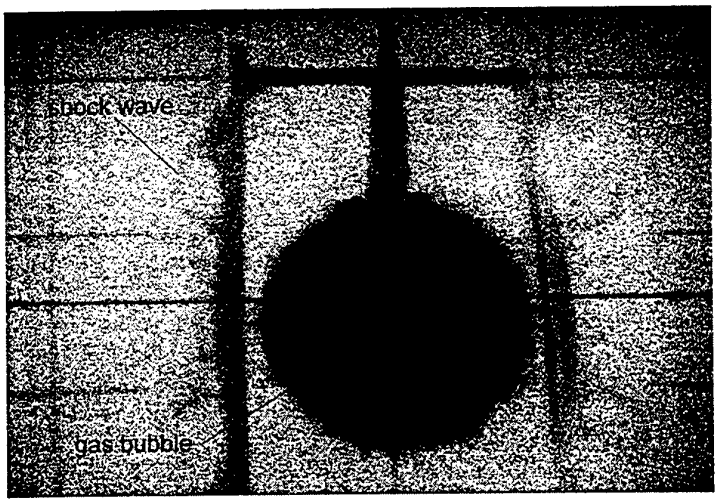

c

Figure 7. The path of the shock wave incident onto, and transmitted from, the steel plate.

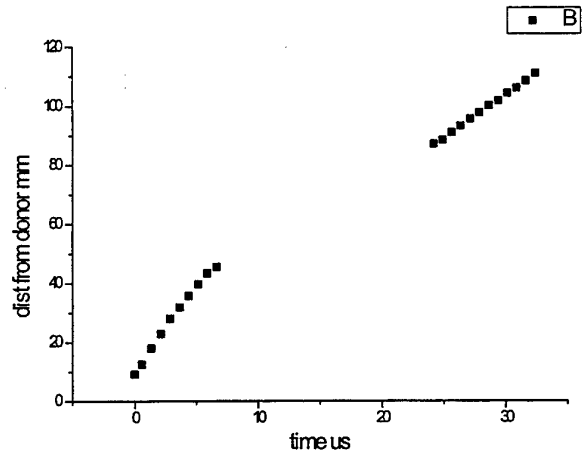

Calculations of the velocity of the shock wave from the gradient of the distance-time curve in Figure 7 show that the average velocity of the shock wave incident onto the plate was 3.9 ± 0.3 $mm/\mu s$ and that of the transmitted wave was 2.9 ± 0.2 $mm/\mu s$. The reduction in the shock wave velocity across the steel plate and the intense reflected wave shown in Figure 6a indicates that poor impedance matching occurs between water and steel, consequently, a significant amount of the shock wave's energy would be expected to be absorbed by the steel plate. The pressures in the water at these points may be calculated from equations (1) and (2) as 4.9 ± 0.6 and 2.1 ± 0.3 GPa respectively which shows that the 6 mm steel plate has attenuated the shock wave by approximately 60 % of its incident value. There is no clear evidence in Figure 6, of additional transmitted shock waves produced by multiple reflections of the shock wave between the bubble and plate.

Estimation of the width of the silhouette of the steel plate from the streak record in a region free of optical distortion, indicates that the plate was dished by 22 mm whereas the degree of dishing of the plate measured after the event was found to be 25.5 mm. Because of the close correlation between these two results, we suggest that the damage to the plate may be attributed to the shock wave alone.

Similar shock wave interaction occurs between the perspex sheet and bubble. The digitised path of the shock wave incident onto and transmitted through the perspex sheet is shown in Figure 8. The almost constant velocity gradient across the perspex sheet indicates that the shock impedance of perspex is more closely matched to that of water.

Figure 8. The path of the shock wave incident onto, and transmitted through, the perspex sheet.

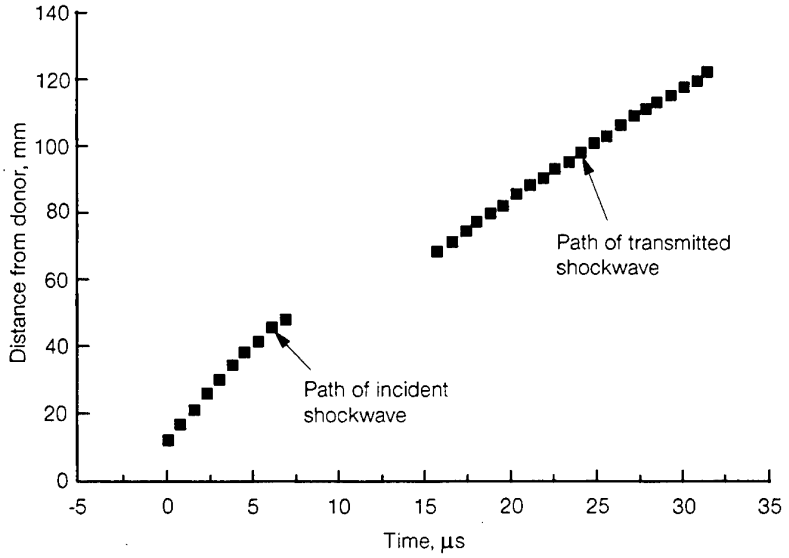

Calculations from the distance-time curve shown in Figure 8 indicate that the average velocity of the shock wave incident onto the perspex sheet is 4.2 ± 0.3 $mm/\mu s$. This velocity is slightly greater than that for the steel plate because the donor is closer to the perspex sheet. The average velocity of the transmitted wave beyond the perspex sheet, was 3.9 ± 0.3 $mm/\mu s$. The pressures calculated at these points were 6.1 ± 0.8 and 5.0 ± 0.7 Gpa respectively which indicate that the perspex sheet has attenuated the shock wave by approximately 20%.

4.3 Initiation of detonation in a Composition B receptor.

Figure 9 illustrates the initiation of detonation in an explosive material by an underwater explosion. A Pentolite donor was suspended in water, approximately 40 mm from a Composition B acceptor and detonated. The streak record shows a shock wave reflected from the acceptor charge 1.5 μs after the incident wave contacts the front of the acceptor whilst detonation breakout is seen to occur 15.2 μs after incident wave contact. At detonation breakout, the donor charge's bubble radius has expanded by 24 mm and has not made contact with the acceptor charge. Both framing and streak records show the luminous detonation front in the acceptor and the development of the shock wave in the water from the detonating acceptor. The linear distance-time response of the reaction in the acceptor charge shown in the streak record indicates that detonation has reached a stable state after detonation breakout.

Figure 9. Streak record (a) and framing records (b & c) showing detonation of the Composition B receptor charge, initiated by the underwater shock wave.

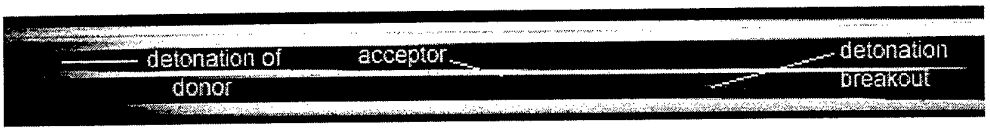

a

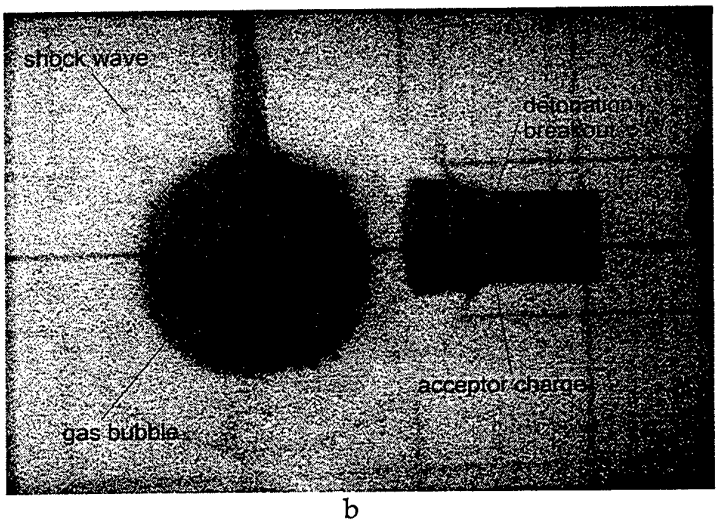

b

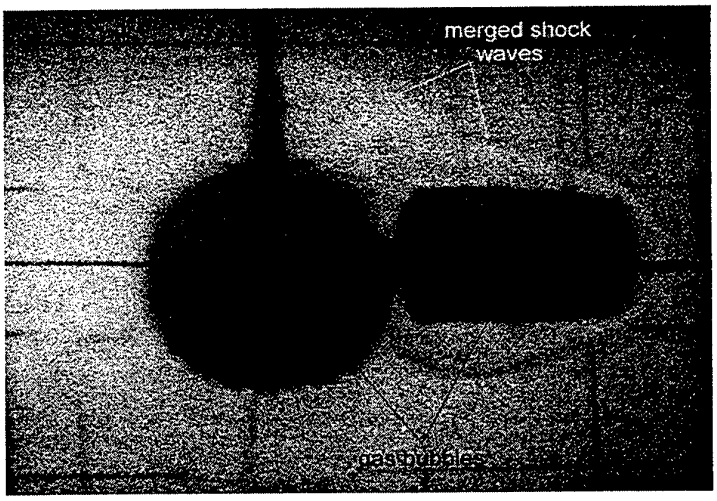

c

The digitised path of the shock wave incident onto and reflected from, the Composition B receptor is shown in Figure 10.

Figure 10. Path of the shock wave interacting with the Composition B acceptor.

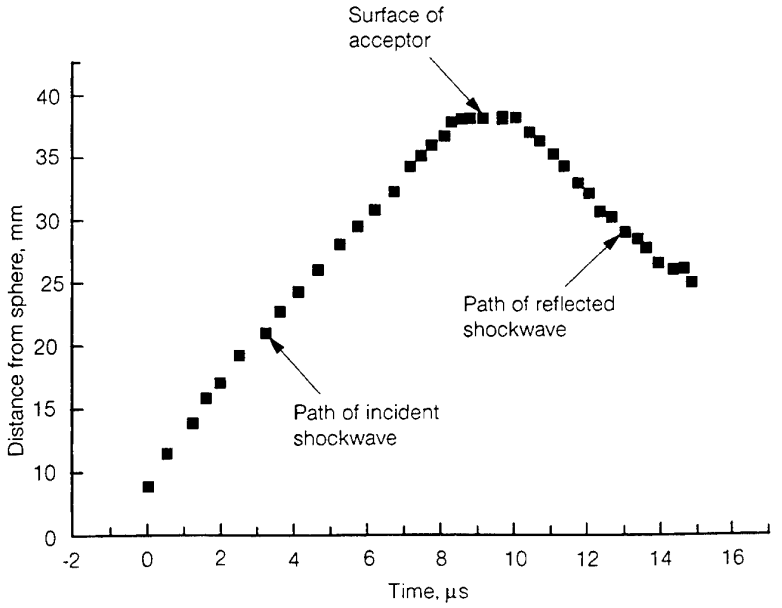

Velocities calculated from Figure 10 were plotted against distance from the surface of the donor and are shown in Figure 11. Reduced distance was not used as the second variable in this plot because on reflection, the properties of the reflected shock wave are determined by the interface between the water and the Composition B acceptor and thus are independent of the dimensions of the donor charge.

Figure 11. Velocity-distance (from donor) path of the shock wave initiating detonation in the Composition B acceptor.

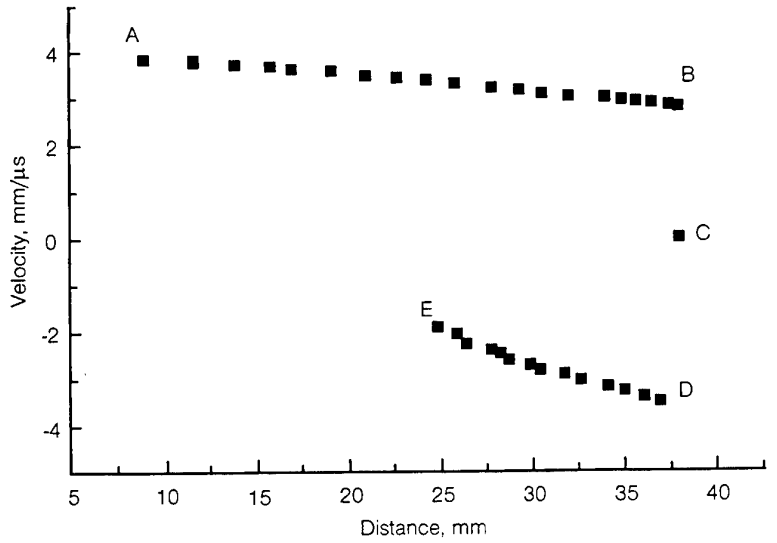

Figure 11 shows the velocity of the shock wave incident onto the acceptor (AB), the acceptor (C) at rest, and the velocity of the reflected shock wave (DE). The velocity of the shock wave incident onto the Composition B acceptor is $2.8 \pm 0.2\ mm/\mu s$.

Using equations (1) and (2), impedance matching techniques and this shock wave velocity, the pressure in the Composition B acceptor may be calculated as 2.7 ± 0.4 GPa, a value close to, but greater, than the detonation pressure threshold (2.5 GPa) for Composition B3 [8], a composition similar to that used in our experiments.

4.4 Initiation of burning in a Composition B receptor.

The initiation of a low order reaction in an explosive acceptor by an underwater explosion is shown in Figure 12. A pentolite donor and Composition B acceptor were positioned approximately 58 mm apart and the donor charge detonated. The framing records show the shock wave interacting with the acceptor but there is no visual evidence that the Composition B acceptor detonated. Neither the characteristic luminous detonation front in the acceptor nor the expanding shock wave from the acceptor was seen to occur in the framing records. The acceptor expands during the passage of the shock wave which indicates that a reaction has taken place within the charge. From the framing camera's records, the rate of expansion is estimated to be 1270 m/s. This value is greater than the rate of expansion (850 m/s) measured by Liddiard and Forbes [2] for the burning of Composition B and is less than the value measured for the expansion of a detonating pentolite sphere (4600 m/s) described earlier in this paper. If the acceptor detonated, its velocity of expansion would be similar too, or greater than that of, the detonating pentolite sphere. Hence, the lower value estimated for the expansion of the Composition B acceptor indicates that the acceptor burnt because the effect lies more closely to a burning reaction than a detonation reaction.

Figure 12. Streak record (a) and framing records (b & c) of a low order reaction in a Composition B acceptor, initiated by an underwater shock wave.

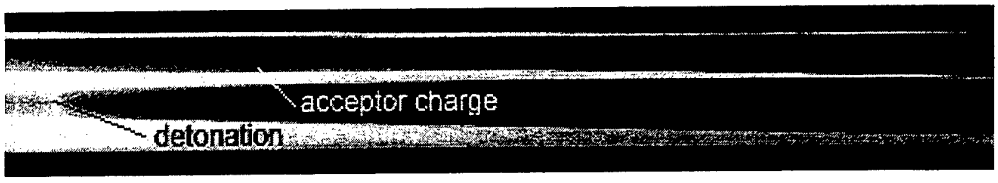

a

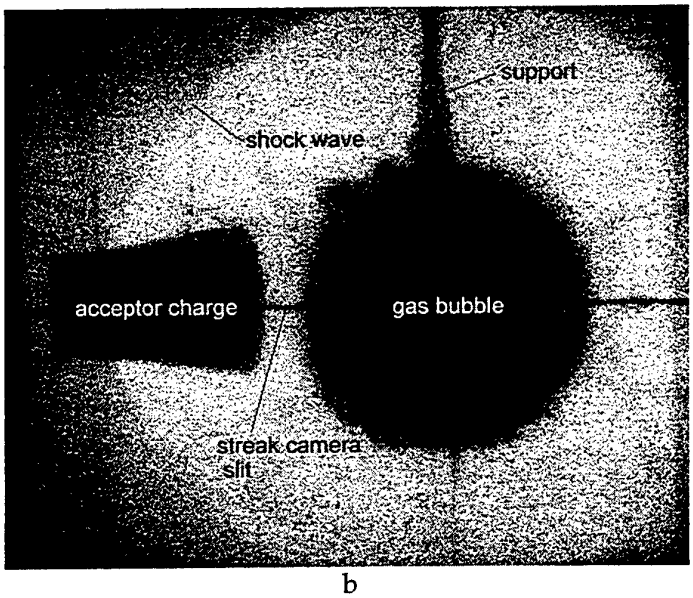

b

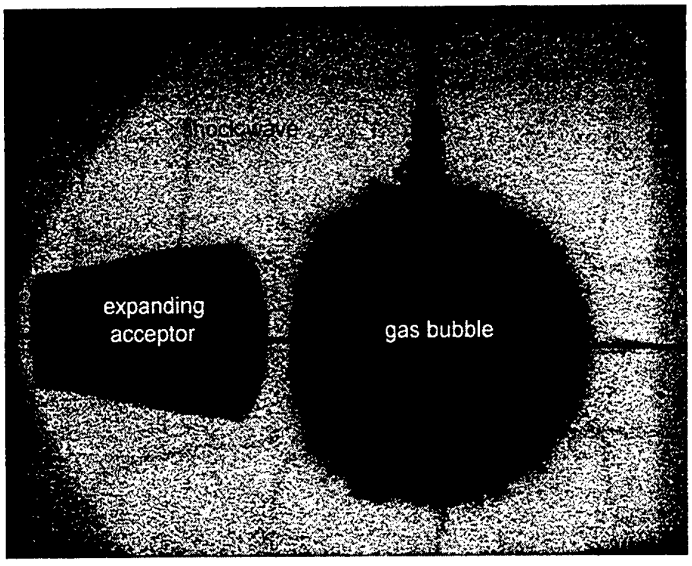

c

The poor exposure of the streak record limited the path over which the shock wave and expanding bubble surface could be tracked and digitised. Consequently, the interaction of the shock wave with the acceptor charge was not recorded. The digitised path of the expanding shock wave over a limited distance is shown in Figure 13. The velocities calculated from the gradients of Figure 13 were plotted against distance from the sphere's surface and are shown in Figure 14.

Figure 13. Path of the underwater shock wave initiating a low order reaction in the Composition B acceptor.

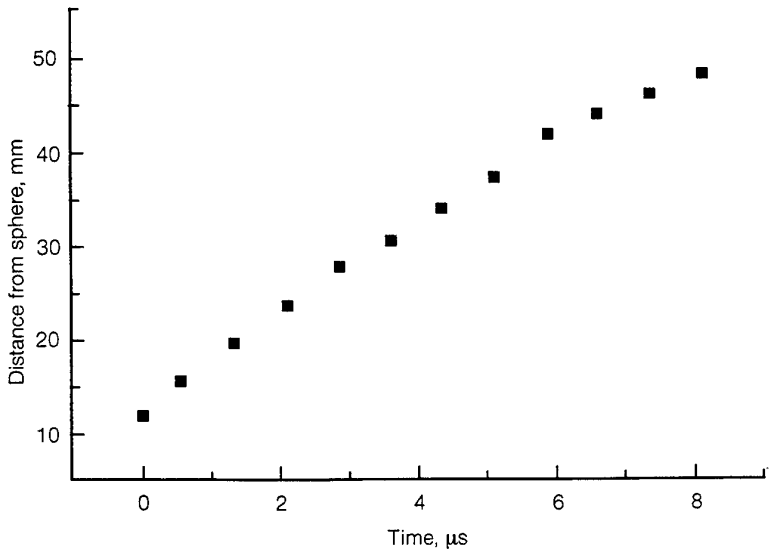

Figure 14. Velocity-distance path of the underwater shock wave that initiates a low order event in the Composition B acceptor.

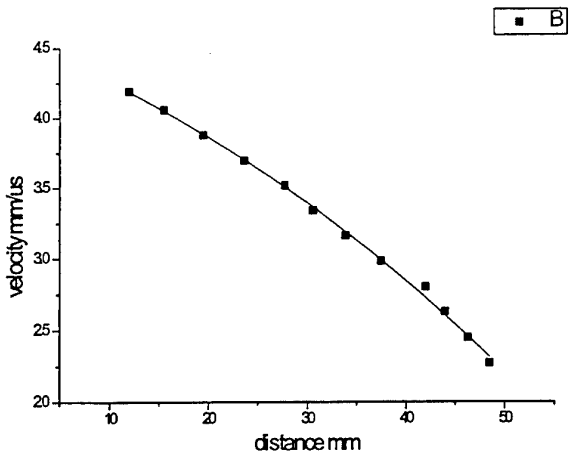

The polynomial of best fit for this curve is given by;

$$U = 4.57 - 0.027s - 0.0004s^2 \qquad (6)$$

where U is the velocity of the shock wave in $mm/\mu s$ and s is the distance from the surface of the sphere in mm. The coefficient of determination for equation (6) is 0.998.

Measurements from the streak record indicate that the separation between donor and acceptor is 58.7 mm. Equation (6) predicts that the velocity of the shock wave at this distance from the donor is 1.6 ± 0.1 $mm/\mu s$. The pressure in the Composition B acceptor due to this underwater shock wave may be calculated from equations (1), (2) and impedance matching techniques as 134 ± 10 MPa, a value that is significantly lower than Composition B3's detonation pressure threshold.

4.5 Perspex shielding effects.

The interaction of an underwater shock wave with a Composition B acceptor shielded by a perspex sheet positioned 31mm from the donor charge is shown in Figure 15. The acceptor was glued to the perspex sheet and supported by adhesive tape, attached from the perspex sheet to the end of the acceptor. The shock wave produced by the detonating donor expanded into the water, propagated through the perspex sheet and into the acceptor charge, after which the characteristic luminous detonation front is visible on the streak record. Detonation breakout occurred 10 μs after initial impact.

The sheet appears to have remained intact during this period and this suggests that the reaction in the acceptor was initiated by the shock wave and not particle impact produced by the disintegrating perspex sheet. Again, the detonation reaction in the acceptor was complete before the expanding detonation products reach the acceptor charge. The digitised path of the shock wave incident onto the perspex sheet is shown in Figure 16 and the variation in velocity with distance is shown in Figure 17.

Figure 15. Streak record (a) and framing records (b & c) showing detonation of a perspex shielded Composition B acceptor.

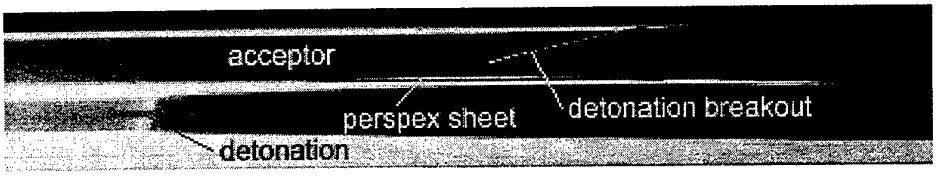

a

b

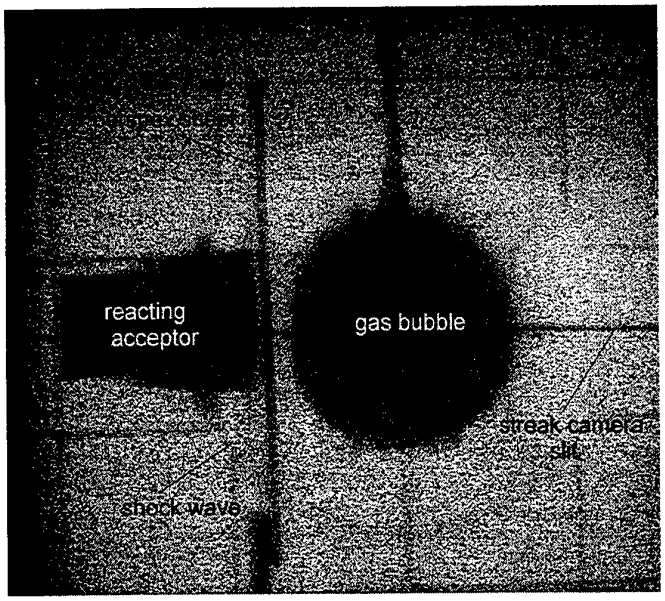

c

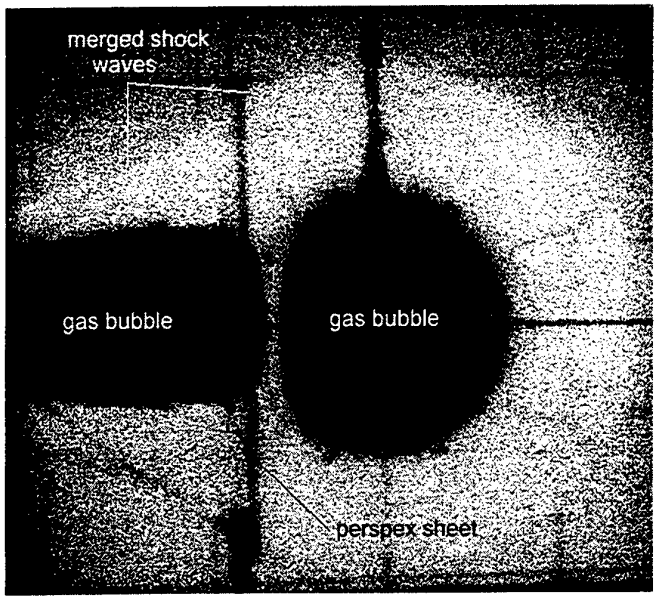

Figure 16. Distance-time plot of the shock wave incident onto the perspex sheet.

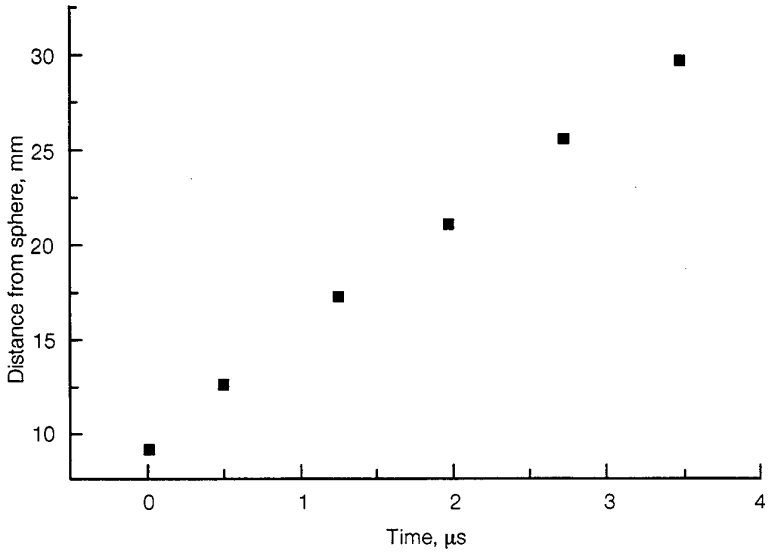

Figure 17. Velocity-distance curve for an underwater shock wave that initiates detonation in a perspex shielded Composition B acceptor.

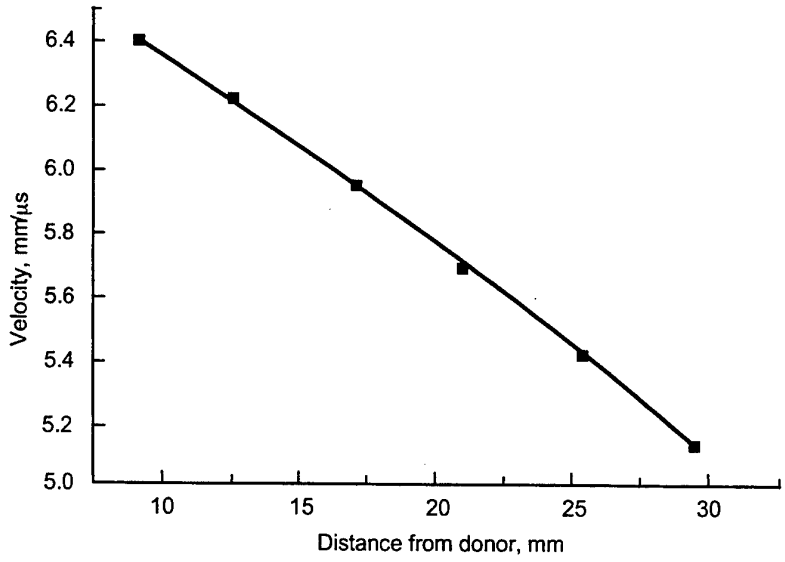

The polynomial of best fit for the curve shown in Figure 17 is given by;

$$U = 4.89 - 0.035s - 0.0003s^2 \qquad (7).$$

The coefficient of determination for equation (7) is 0.999.

For the measured separation between donor and perspex sheet of 31 mm, equation (7) indicates that the velocity of the shock wave at the sheet is $3.7 \pm 0.2\ mm/\mu s$. Using methods similar to that described above, the pressure within the Composition B acceptor may be calculated as 5.6 ± 0.8 GPa.

4.6 Compilation of velocity/reduced distance results.

The variation in velocity with reduced distance from the donor for the shock waves described earlier in this paper is shown in the compilation of results in Figure 18. This Figure shows curves, the gradients of which fall into two distinct sets, with the difference between their initial velocities of approximately 1000 m/s. These results are somewhat unexpected because this effect could be produced if pentolite has more than one detonation state, each with a different velocity of detonation. Under these circumstances, and depending on the conditions of the experiment, it would be possible for shock waves of different initial velocities to be produced at the explosive/water interface. However, as pentolite is known to have one detonation state and as the method of initiation, the casting technique, the quality of the pentolite charge and the experimental technique was identical for each experiment, the differences between the initial velocities of the shock waves cannot be simply explained.

The spread of initial velocities and the gradients may of course, be a function of the correction factor applied to curves 1 and 2 in Figure 18 to compensate for the difference between measured and reference velocity of detonation of Composition B. The true correction factor may not be constant as first assumed (0.7) for the turbine speed of 480 μs but linear, such that the rate of change in velocity of the shock wave with (reduced) distance is less.

Figure 18. Compilation of the results showing the variation in Velocity with Reduced Distance from the donor for shock waves investigated in earlier experiments.

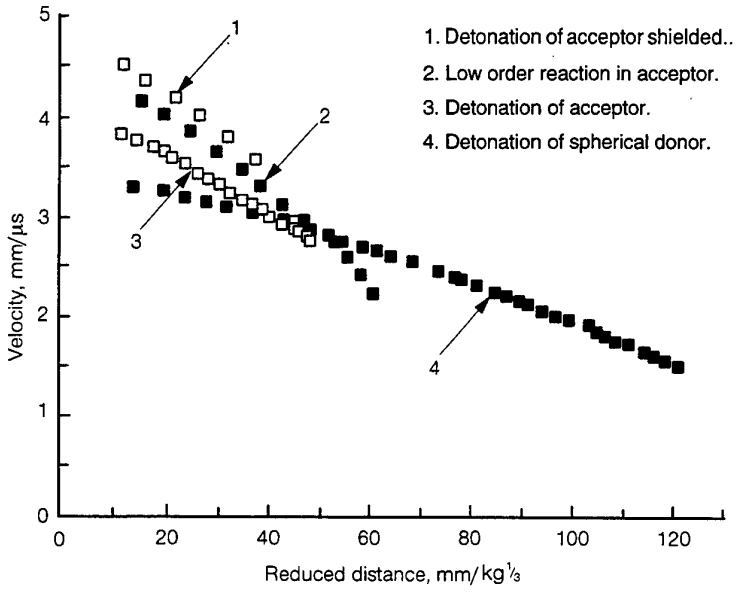

When each set of results is considered in isolation, the results are reasonable. All show an initial high velocity of the shock wave with a rapid reduction towards water's acoustic velocity, the pressures within the Composition B acceptors, calculated from experimental observations, could be expected to produce the effects they achieved and whilst a pressure of 5.6 $\pm$0.8 Gpa predicted for a perspex shielded acceptor is somewhat high, it is not unreasonable given the simple methods used to analyse the results from these experiments.

Despite the above variation in the sets of results, a polynomial curve of best fit to describe the data in Figure 18 is given by;

$$U = 4.43 - 0.036R + 0.0001R^2, \qquad (8)$$

the coefficient of determination for this curve is 0.91.

A summary of predicted pressures within the Composition B receptors and the observed effect of the interaction of an underwater shock wave on the receptors is shown in Table 2.

Table 2. Predicted and observed effects of the interaction of shock waves with Composition B receptors.

Experiment described in section:	Predicted pressure in Composition B GPa	Result
4.3	2.7 ± 0.4	Detonation
4.4	0.134 ± 0.01	Burning
4.5	5.6 ± 0.8	Detonation

Detonation occurred in each case where the predicted pressures within the receptor exceeded the detonation pressure of Composition B (2.5 GPa).

5. Conclusions.

Experimental studies have shown that in the near-field, close by an underwater explosion;

1. the velocity of the shock wave falls more quickly than that predicted by the inverse square law, consequently, the experimental curve of best fit described by equation (8) is suitable to describe the variation in shock wave velocity with reduced distance,
2. damage sustained to simple structures and the initiation of both detonation and burning reactions to Composition B may be attributed to the passage of the shock wave alone and
3. results obtained from impedance matching techniques used to predict pressures within Composition B acceptors suggest that peak pressures are the critical initiation parameter of an underwater shock wave.

6. References.

1. Sternberg, H.M., Walker, W.A., (1971). Calculated Flow and Energy Distribution Following Underwater Detonation of a Pentolite Sphere, The Physics of Fluids, Vol.14, Number 9.

2. Liddiard, T.P., Forbes, J.W., (1987). A Summary Report of the Modified Gap Test and the Underwater Sensitivity Test, NSWC TR 86-350, Naval Surface Warfare Centre, Dahlgren, Virginia.

3. Chung, M.J., McQueen, D., McVay,.L.,(1996). Initiation of Detonation in Composition B by an Underwater Shock Wave, DSTO-TR-0273, Melbourne, Victoria.

4. Duvall, G.F., Fowles, R. (1963). Chapter 9, High Pressure Physics and Chemistry, Vol. 2, R. S. Bradley (Ed.), Academic Press, London.

5. Rice, M.H., Walsh, J.M., (1957). Equation of State of Water to 250 Kilobars, Journal of Chem. Phy., Vol. 26, No4, pp 824-830.

6. Mader, C.L.,(1979). Numerical Modeling of Detonations, University of California Press, Berkeley.

7. Cole, R.H., (1948). Underwater Explosions, Princeton University Press, Princeton, New Jersey.

8. Price, D., *et al.* (1974). The NOL Large Scale Gap Test III. Compilation of Unclassified Data and Supplementary Information for Interpretation of Results, NOLTP74-40, Naval Ordnance Laboratory, White Oak, Maryland.

DISTRIBUTION LIST

Underwater Blast Effects on Simple Structures, Shielded and Bare Explosive Materials

Michael Chung and Trevor Kinsey

AUSTRALIA

DEFENCE ORGANISATION

Task Sponsor **Minehunter Coastal Project**

S&T Program

Chief Defence Scientist
FAS Science Policy
AS Science Corporate Management
} shared copy

Director General Science Policy Development
Counsellor Defence Science, London (Doc Data Sheet)
Counsellor Defence Science, Washington (Doc Data Sheet)
Scientific Adviser to MRDC Thailand (Doc Data Sheet)
Director General Scientific Advisers and Trials/Scientific Adviser Policy and Command (shared copy)
Navy Scientific Adviser
Scientific Adviser - Army (Doc Data Sheet and distribution list only)
Air Force Scientific Adviser
Director Trials

Aeronautical and Maritime Research Laboratory
Director

Chief of Weapon Systems Division
Research Leader: David Thomson, RLMWS
Head, Terminal Effects: David Ritzel
Task Manager
Author(s): Michael Chung & Trevor Kinsey

DSTO Library
Library Fishermens Bend
Library Maribyrnong
Library Salisbury (2 copies)
Australian Archives
Library, MOD, Pyrmont (Doc Data sheet only)
Library, MOD, HMAS Stirling

Capability Development Division
Director General Maritime Development
Director General Land Development (Doc Data Sheet only)
Director General C3I Development (Doc Data Sheet only)

Navy

SO (Science), Director of Naval Warfare, Maritime Headquarters Annex, Garden Island, NSW 2000
MCP, Project Director, Campbell Park Offices, Canberra (2 copies)
DNW, Maritime Headquarters, Potts Point, Sydney
DARMENG-Navy, Campbell Park Offices, Canberra

Army

ABCA Office, G-1-34, Russell Offices, Canberra (4 copies)
SO (Science), DJFHQ(L), MILPO Enoggera, Queensland 4051 (Doc Data Sheet only)
NAPOC QWG Engineer NBCD c/- DENGRS-A, HQ Engineer Centre Liverpool Military Area, NSW 2174 (Doc Data Sheet only)

Air Force

Intelligence Program

DGSTA Defence Intelligence Organisation

Acquisitions Program

Corporate Support Program (libraries)

OIC TRS, Defence Regional Library, Canberra
Officer in Charge, Document Exchange Centre (DEC), 1 copy
*US Defence Technical Information Center, 2 copies
*UK Defence Research Information Centre, 2 copies
*Canada Defence Scientific Information Service, 1 copy
*NZ Defence Information Centre, 1 copy
National Library of Australia, 1 copy

AUSTRALIAN ORDNANCE COUNCIL

Secretary, Campbell Park Offices, Canberra

UNIVERSITIES AND COLLEGES

Australian Defence Force Academy
Library
Head of Aerospace and Mechanical Engineering
Deakin University, Serials Section (M list), Deakin University Library, Geelong, 3217
Senior Librarian, Hargrave Library, Monash University
Librarian, Flinders University

OTHER ORGANISATIONS

NASA (Canberra)
AGPS

OUTSIDE AUSTRALIA

ABSTRACTING AND INFORMATION ORGANISATIONS

INSPEC: Acquisitions Section Institution of Electrical Engineers
Library, Chemical Abstracts Reference Service
Engineering Societies Library, US
Materials Information, Cambridge Scientific Abstracts, US
Documents Librarian, The Center for Research Libraries, US

INFORMATION EXCHANGE AGREEMENT PARTNERS

Acquisitions Unit, Science Reference and Information Service, UK
Library - Exchange Desk, National Institute of Standards and Technology, US

SPARES (10 copies)

Total number of copies: 67

DEFENCE SCIENCE AND TECHNOLOGY ORGANISATION
DOCUMENT CONTROL DATA

1. PRIVACY MARKING/CAVEAT (OF DOCUMENT)

2. TITLE

Investigation into the Effects of Underwater Shock Waves on Simple Structures, Shielded and Bare Explosive Materials

3. SECURITY CLASSIFICATION (FOR UNCLASSIFIED REPORTS THAT ARE LIMITED RELEASE USE (L) NEXT TO DOCUMENT CLASSIFICATION)

Document	(U)
Title	(U)
Abstract	(U)

4. AUTHOR(S)

Michael Chung and Trevor Kinsey

5. CORPORATE AUTHOR

Aeronautical and Maritime Research Laboratory
PO Box 4331
Melbourne Vic 3001 Australia

6a. DSTO NUMBER	6b. AR NUMBER	6c. TYPE OF REPORT	7. DOCUMENT DATE
DSTO-RR-0134	AR-010-571	Research Report	June 1998

8. FILE NUMBER	9. TASK NUMBER	10. TASK SPONSOR	11. NO. OF PAGES	12. NO. OF REFERENCES
510/207/0316	NAV 94/203	MMCPO	25	8

13. DOWNGRADING/DELIMITING INSTRUCTIONS

14. RELEASE AUTHORITY

Chief, Weapons Systems Division

15. SECONDARY RELEASE STATEMENT OF THIS DOCUMENT

Approved for public release

OVERSEAS ENQUIRIES OUTSIDE STATED LIMITATIONS SHOULD BE REFERRED THROUGH DOCUMENT EXCHANGE CENTRE, DIS NETWORK OFFICE, DEPT OF DEFENCE, CAMPBELL PARK OFFICES, CANBERRA ACT 2600

16. DELIBERATE ANNOUNCEMENT

No Limitations

17. CASUAL ANNOUNCEMENT Yes

18. DEFTEST DESCRIPTORS

Shockwaves, Underwater detonation, Naval mines, Explosives

19. ABSTRACT

The detonation of an underwater charge creates a shock wave and a bubble of gaseous products at high temperature and pressure. At greater ranges, the shock wave and bubble become separated and their effects on structures may be studied separately. However, close to the point of detonation, in the regions typically used for sea-mine neutralisation, the shock wave and bubble lie in close proximity and their relative importance in the neutralisation process is not known. A series of scaled experiments to visualise the early development of the shock wave and bubble, and their interactions with an explosive and with simple structures were devised. These experiments used spherical pentolite charges and cylindrical Composition B charges as the donor and acceptor charges respectively. Both charges were suspended in a small, transparent water-filled tank and the effects of the exploding donor recorded by a Cordin rotating mirror camera.